Separation Science and Technology
Publication details, including instructions for authors and subscription information:
http://www.informaworld.com/smpp/title~content=t713708471

The Effect of Floc Size and Structure on Specific Cake Resistance and Compressibility in Dead-End Microfiltration

S. A. Lee[a]; A. G. Fane[a]; R. Amal[a]; T. D. Waite[b]
[a] School of Chemical Engineering and Industrial Chemistry, The University of New South Wales, Sydney, NSW, Australia [b] School of Civil and Environmental Engineering, The University of New South Wales, Sydney, NSW, Australia

Online publication date: 20 February 2003

To cite this Article Lee, S. A. , Fane, A. G. , Amal, R. and Waite, T. D.(2003) 'The Effect of Floc Size and Structure on Specific Cake Resistance and Compressibility in Dead-End Microfiltration', Separation Science and Technology, 38: 4, 869 — 887
To link to this Article: DOI: 10.1081/SS-120017631
URL: http://dx.doi.org/10.1081/SS-120017631

MARCEL DEKKER, INC. • 270 MADISON AVENUE • NEW YORK, NY 10016

SEPARATION SCIENCE AND TECHNOLOGY
Vol. 38, No. 4, pp. 869–887, 2003

The Effect of Floc Size and Structure on Specific Cake Resistance and Compressibility in Dead-End Microfiltration

S. A. Lee,[1] A. G. Fane,[1,*] R. Amal,[1] and T. D. Waite[2]

[1]School of Chemical Engineering and Industrial Chemistry and [2]School of Civil and Environmental Engineering, The University of New South Wales, Sydney, NSW, Australia

ABSTRACT

The effects of floc properties (size and structure) on specific cake resistance and compressibility of cakes formed by dead-end MF were investigated. Hematite particles of primary size 70 nm were flocculated in the presence of KCl and stirring and the resultant flocs were characterized in terms of floc size and fractal dimension. The results showed that larger flocs (ca 40 μm diameter) produced filter cakes of lower specific resistances and floc structural effects were more significant for smaller floc (ca 10 μm), with higher specific resistance for cakes formed from more compact flocs. These observations are explained by the balance of inter- and intra-floc flow and are in accord with a modified Carman-Kozeny

*Correspondence: A. G. Fane, School of Chemical Engineering and Industrial Chemistry, The University of New South Wales, Sydney 2052, NSW, Australia; E-mail: a.fane@unsw.edu.au.

DOI: 10.1081/SS-120017631 0149-6395 (Print); 1520-5754 (Online)

relationship, which incorporates fractal dimension. Cake compressibility is strongly related to transmembrane pressure (TMP) particularly for smaller floc sizes. At low TMP (< 10 kPa) the estimated cake-averaged porosity is almost independent of floc size but at raised TMP (> 60 kPa) the porosity is strongly size dependent with higher porosities for larger floc. For the smaller flocs, cakes formed from the less compact floc (smaller fractal dimension) show greater tendency to compression.

Key Words: Membrane technology; Fouling; Flocculation; Compression; Floc structure.

INTRODUCTION

The performance of microfiltration (MF) in water and wastewater treatment can be significantly enhanced by chemical addition. It is now common practice to add flocculents to the feed to increase the removal of natural organic matter from raw water[1] and improve the flux if fine colloids are present.[2] The tendency is also to use dead-end MF or UF rather than pumped crossflow to reduce energy.[1,3] This dead-end membrane filtration of flocculated solids provides a contrast to the conventional MF application where crossflow limits deposition and the feed may be modified by surface shear. In both crossflow and dead-end operation the flux is given by,

$$J = \frac{\Delta P}{\mu(R_m + R_c)} \tag{1}$$

The cake resistance is related to the cake load (m') and the specific cake resistance (α_c), by,

$$R_c = m'\alpha_c \tag{2}$$

In dead-end operation m' and R_c grow with time so that flux drops (at constant ΔP) or ΔP rises at constant flux. Furthermore in dead-end filtration the cake resistance tends to dominate so that the filtration cycle depends on the specific resistance of the cake, which in turn depends on the "structure" of the cake. For rigid spheres the well-known Carman-Kozeny equation[4] relates α_c to particle size (d_p) and cake porosity (ε_c),

$$\alpha_c = \frac{36K''(1-\varepsilon_c)}{\rho_p d_p^2 \varepsilon_c^3} \tag{3}$$

Where K'' is the empirical Kozeny constant. For typical porosities (0.3 to 0.5), K'' is about 5.0 but for high porosity K'' increases.[5] With flocculated aggregates the situation is different because the aggregates tend to be porous, which could provide added permeability to the cake. The implication of this is that the specific resistance of the deposit can be influenced by the properties (size and porosity) of the floc in the feed, and that membrane performance can be enhanced by optimizing floc formation.[6,7]

The structural character of flocculated aggregates can be related to the mass fractal dimension, d_F, of the floc by [floc mass $\propto$ (floc size)^{dF}], where $d_F = 3$ defines a sphere and $d_F = 2$ a sheet and typical flocs have d_F values in the range 1.7 to 2.5. The aggregate porosity is related to the primary particle size (radius r_p), the aggregate size (r_a), and the fractal dimension by,[8]

$$\varepsilon_a = 1 - \left(\frac{r_a}{r_p}\right)^{dF-3} \tag{4}$$

This relationship shows that for a given d_F the aggregate porosity (ε_a) tends to increase as the size increases. Cakes formed of particles of $d_F = 3$ will have a porosity equivalent to the random packing of hard spheres (ε_s, in the range 0.3 to 0.4) whereas cakes formed of aggregates would tend to have porosities lying between the extremes of ε_s and ε_a, providing the aggregates do not collapse.

An important issue is the extent to which the fractal character of aggregates is maintained in the filter cake. Khatib et al.[9] studied chemically assisted UF of raw water and suggested that the fractal properties of the aggregates formed may have influenced the membrane filtration behavior. In previous work[10] we observed that filter cakes generated from hematite flocs formed in a low salt environment (reaction limited aggregation, RLA) have α_c values an order of magnitude higher than cakes generated from flocs formed in a high salt environment (diffusion limited aggregation, DLA). These results are consistent with the understanding that RLA leads to compact floc (higher d_F) and DLA produces more open floc (lower d_F). The fractal structure of cakes formed by filtration of aggregates has been confirmed[11,12] but Antelmi et al.,[13] using in situ monitoring by small-angle-neutron scattering, found that pressure-induced cake collapse can obscure the original aggregate structure. The extent of this effect depended on the applied pressure (they used 20 to 400 kPa) and the aggregate strength (they used relatively weak latex aggregates).

If the fractal nature of the floc is preserved in the filtration process the Carman-Kozeny equation can be modified[14] to give,

$$\alpha_c \propto \frac{1}{\left(\frac{d_{floc}}{d_p}\right)^{3-dF} \times \left(1 - \frac{1}{\left(\frac{d_{floc}}{d_p}\right)^{3-dF}}\right)^3} \tag{5}$$

From Eq. (5) it is possible to show the qualitative relationship between the specific cake resistance and the floc size and fractal dimension (Fig. 1). These calculations suggest that fractal dimension is more important for smaller floc, presumably because the smaller floc produce more resistant cakes that are benefited by floc permeabilty.

In this study we have microfiltered suspensions of hematite aggregates prepared under controlled conditions to give a range of floc size and structures characterized by fractal dimension. While the aggregation process does not

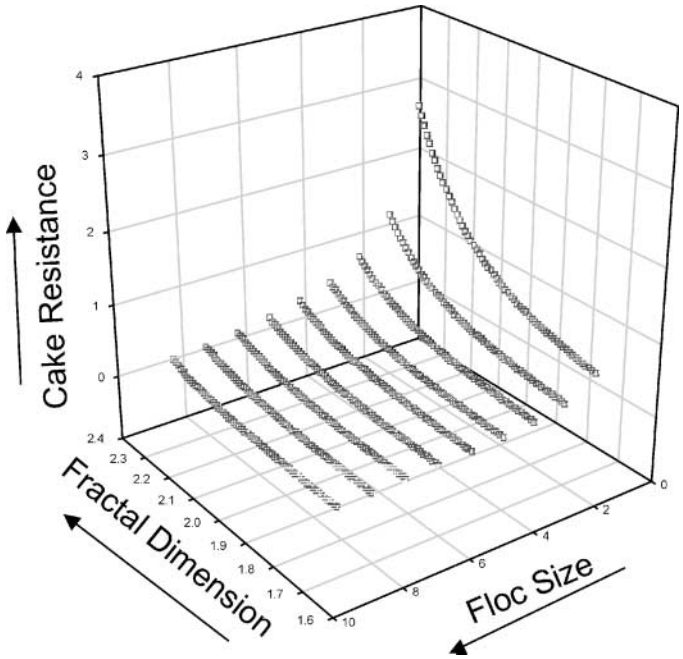

Figure 1. Relationship between specific cake resistance, floc size, and fractal dimension, based on modified Carman-Kozeny relationship.[14]

allow precise control of the floc size and $d_{F,}$ we have been able to examine the interplay of these parameters in the magnitude of the specific resistance and compressibilty of the generated filter cakes.

EXPERIMENTAL

Floc Preparation

The first step in floc preparation was the production of colloidal hematite (α-Fe_2O_3) by hydrolysis of $FeCl_3$ at 100 °C.[15,16] The particles produced were thoroughly washed and then redispersed in MilliQ water and the concentration measured using atomic absorption spectrometry. Suspensions were stored at pH 4 in a refrigerator. Potassium chloride was used for particle destabilization and 0.1 N HCl and NaOH solutions were used to control solution pH, the chemicals used were AR grade. All aqueous salt solutions were made using MilliQ water ($>$ 18 MΩ/cm) and prefiltered using a Millipore GVWP membrane before use.

The hematite particles (measured size d_p ~70 nm) were aggregated in KCl solution in the presence of shear provided by stirring. The range of KCl concentrations used was from 50 mM to 150 mM, which covered both reaction-limited aggregation (RLA) and diffusion-limited aggregation (DLA) mechanisms.[10] In order to prepare 200 mL of hematite floc suspension, 100 mL of KCl solution with double the desired concentration of KCl was prepared and pH adjusted to 4. Then 100 mL of hematite suspension of known hematite concentration (20 ppm Fe) and of pH 4 was prepared and sonicated for at least 10 minutes to break up any spontaneously flocculated particles. The hematite suspension was slowly added to the KCl solution in a 500 mL glass beaker and mixing applied at a controlled rate using an overhead stirrer with blade size of 1 cm in height by 5 cm in width. To obtain a range of floc sizes and structures flocculation was performed at different mixing speeds (30 to 180 rpm) and for different flocculation times (20 to 90 minutes).

Floc Characterization

A Malvern Mastersizer E (Malvern Instruments, UK) was used to measure the floc size distribution and structure. The Mastersizer is a static small-angle laser light scattering (SALLS) instrument designed to characterize particles of sizes ranging from submicron to 600 μm using three different lens. The 100 mm lens, covering 0.5 to 180 μm size range, was

used in this study. Particle size distribution can be estimated by measuring the scattered intensity (I) at a series of scattering angles (θ) The light scattering data obtained were also used to obtain the fractal dimension, $d_{F,}$ by measuring the slope of the log I versus log q plots [where $q = (4\pi n/\lambda)\sin\theta/2$] in the fractal scattering regime.[17] Here q is the change of unit vector of incident and scattered light, n is refractive index of the medium in vacuum, and λ is the wavelength of the incident light (632.8 nm).

Dead-End Microfiltration

The specific cake resistance and compressibility of the filter cake was determined by dead-end microfiltration. Hydrophilic Millipore GVWP membranes (hydrophilized PVDF, nominal pore size 0.22 μm) were used for all the filtration experiments. Most experiments used a membrane area of 15.2 cm^2 in a 110 mL perspex cell, but some experiments used an area of 0.8 cm^2 in a Swinnex 13 membrane housing made by Millipore. Membranes were washed thoroughly after being placed in the membrane housing. Nitrogen gas was used to apply constant pressure and the feed suspension was not stirred in the membrane filtration housing.

The specific resistances of cakes formed from hematite flocs were obtained by measuring the permeate volume (V) as a function of filtration time (t) for various suspension and operating conditions and plotting according to cake filtration theory as t/V versus V,

$$\frac{t}{V} = \frac{\mu\alpha_c C}{2A^2\Delta P}V + \frac{R_m\mu}{A\Delta P} \tag{6}$$

where μ is viscosity of the medium, C is the particle concentration, A is the filter area, ΔP corresponds to the transmembrane pressure (TMP), and R_m is the membrane resistance. α_c is obtained from the slope of the plot. The experimental setup for measurement of specific cake resistance during cake formation is shown in Fig. 2(a).

In order to measure cake compressibility, dead-end MF was performed in two steps. A reservoir (1500 mL) containing a known amount of flocculated hematite suspension was connected to the membrane cell and hematite suspension was filtered through the GVWP membrane at low TMP. The driving force for the hematite suspension filtration was either gravity (for the 15.2 cm^2 membrane) or slow pumping from the permeate side (for the 0.8 cm^2 membrane). The flux was nearly constant and similar to that of the virgin membrane at the low TMPs used [gravity: 7 kPa, pumping: 20 kPa, Fig. 2(b)]. When the reservoir was empty, and the membrane cell was still full of

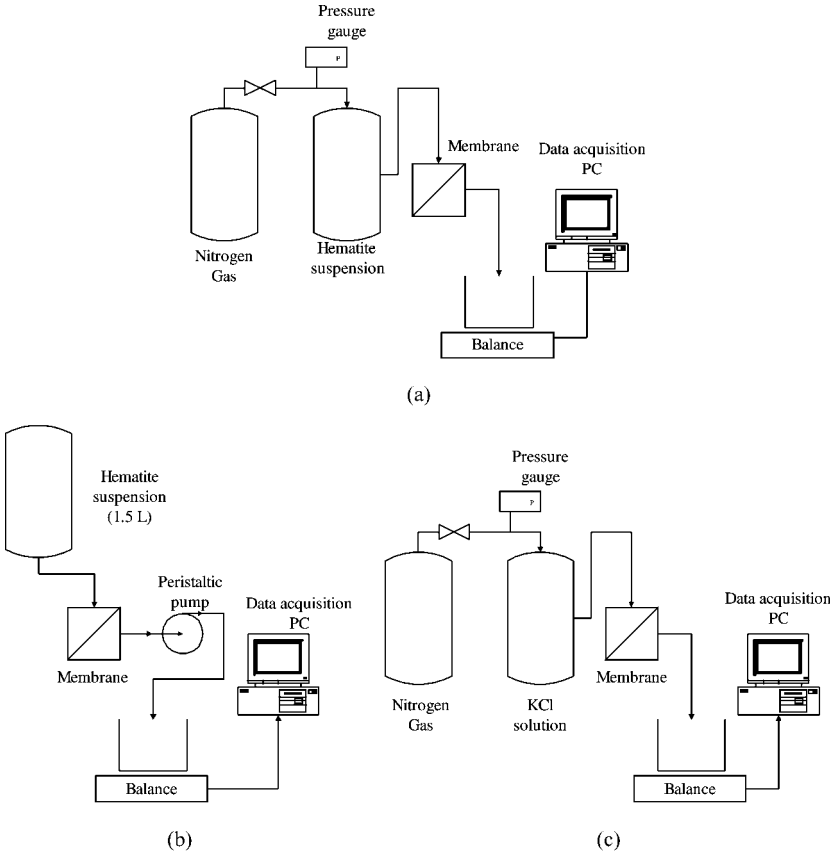

Figure 2. Schematic diagrams of dead-end microfiltration facilities. (a) Setup to measure specific cake resistance during cake formation. (b) First step to form a cake made of hematite flocs under low TMP. (c) Second step to induce cake compression using stepwise elevation of gas pressure.

solution, it was replaced by a new reservoir containing 1000 mL of particle-free KCl solution of the same concentration and pH as that of the hematite suspension. Compression of the cake was induced by flow of the salt solution through the preformed cake at higher TMP (>cake formation pressure) and flux decline was monitored. Nitrogen pressure was increased step by step when the flux value became steady at a given TMP (Fig. 2(c)). At each step the flux increased then declined, enabling determination of the new value of R_c from Eq. (1). The specific cake resistance, α_c, was then calculated using Eq. (2)

since cake load, m', was known. The compressibility of the hematite cake was obtained from the slope of log α vs. log ΔP_c according to the relationship,

$$\alpha_c = \alpha_0 \Delta P_C^n \tag{7}$$

where n is the cake compressibility factor and α_0 is an empirical constant that represents specific cake resistance in the absence of pressure difference.[18] The pressure difference used, $\Delta P_{c,}$ was the pressure difference across the cake (TMP $-$ ΔP_m); this allows for the fact that at the lowest pressures used ($<$ 10kPa) the cake and membrane resistances were of similar magnitude.

The above approach is similar to the classical compression-permeability cell measurement where a preformed cake is compressed. An alternative is conventional constant pressure cake filtration at a series of pressures and plotting the data as t/V vs. V (Eq. 6) to obtain α vs. TMP. However, in practice dead-end MF is usually performed at a constant (modest) flux which leads to a gradually changing TMP as the cake forms. We have used this approach previously[19] to analyze pilot plant data, but the effect of pressure can be obscured. Each scenario (pressurization of preformed cakes, cake formation at different fixed pressures, cake formation at fixed fluxes) will lead to a different history of flux and imposed drag forces. Cake formation at fixed pressure tends to lead to compression of the initial cake layers, and cake formation at fixed flux experiences a range of TMPs in a given cycle. We have selected the pressurization of a preformed cake to get a less ambiguous picture of the effect of pressure per se on the deposited floc.

RESULTS AND DISCUSSION

Floc Properties

The size distribution and structure of floc were measured using SALLS prior to filtration. After 5 to 20 minutes of flocculation flocs became evident depending on salt concentration and stirring speed. When the floc size reached steady state or approached the desired size the stirring was ceased to stop flocculation. Floc size was measured immediately before filtration because spontaneous flocculation and floc growth may occur after the cessation of shear force. However the measured changes in floc properties after the stirring stopped were minimal. In addition, no primary particles or flocs smaller than about 1 μm were detected before filtration. Figure 3 shows typical floc growth histories. To produce a range of floc properties both salt concentration and mixing speed were varied; Table 1 gives examples of the conditions used and

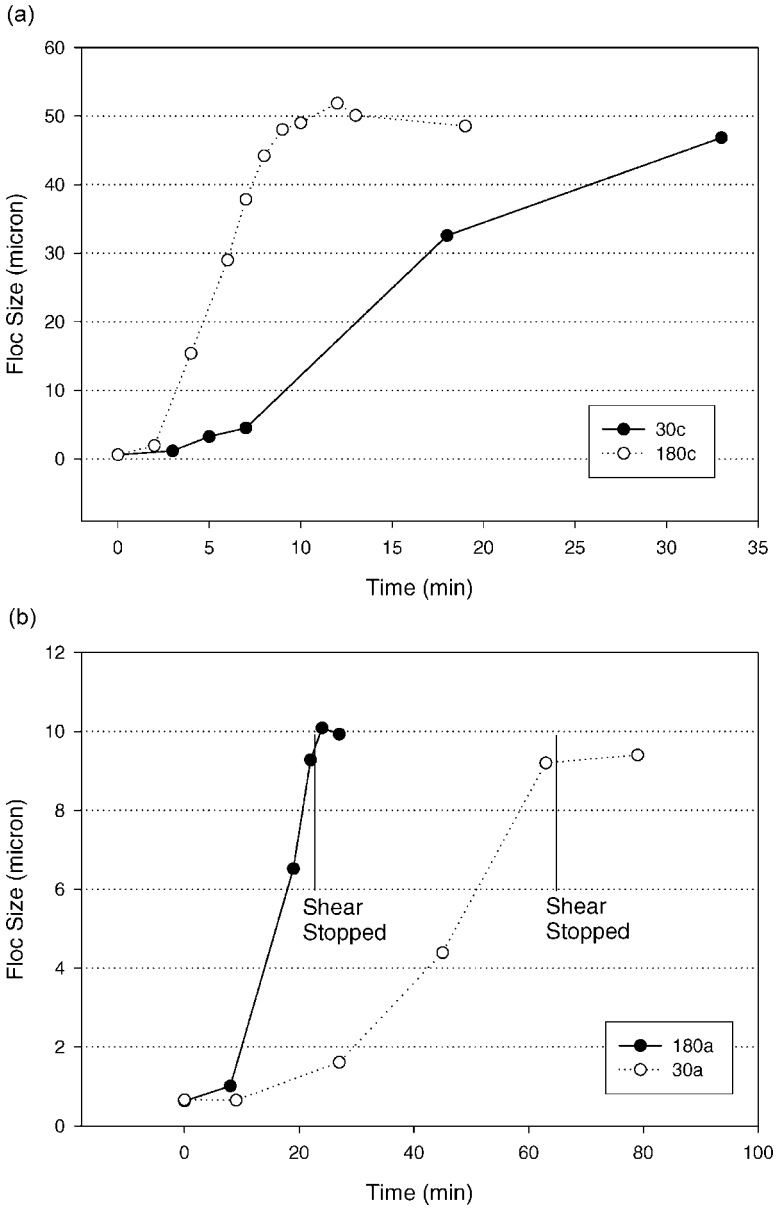

Figure 3. Floc evolution data. (a) Production of large flocs (b) Production of small flocs.

Table 1. Floc properties, median size (d_{50}), size distribution parameter (d_{50}/d_{10}), and compactness for various conditions of mixing speed and salt concentration.

Sample no.	Mixing speed (rpm)	[KCl], mM	d50 (μm)	d50/d10	Compactness or dF
30a	30	100	10.27	2.89	1.83
30b	30	100	13.89	3.56	1.85
30c	30	100	46.85	4.77	Low
90a	90	100	8.28	3.44	2.18
180a	180	100	9.93	3.92	2.21
180b	180	100	8.05	3.76	2.25
180c	180	100	48.54	1.95	High
180d	180	50	40.60	2.03	High

the typical resultant floc properties. Flocs in two size ranges were produced, large flocs which were about 40–50 μm and small flocs about 10 μm. Filtration results of those flocs were analyzed and are shown in Fig. 3 and Fig. 8. It should be noted that the nature of feed preparation was such that minor variations in feed properties were inevitable. However, floc were consistently prepared with d_{50} values in the range 10 to 15 μm and d_F values ± 0.1. The parameters required for calculation of α_c were volume, time, and pressure and all were known within $\pm 1\%$.

The flocs produced had single mode size distributions, unlike some of the bimodal floc measured in our earlier work.[10] The ratio of d_{50}/d_{10} shown in Table 1 characterizes the floc size distributions, which were relatively narrow. This implies that there would be little filtration of fines within the interstices of the deposited cake. Table 1 also shows measured d_F of the smaller floc. For the larger flocs the estimation of d_F was rather subjective due to nonlinearity in the log I vs. log q plots and the compactness is defined qualitatively as low to high based on the flocculation conditions.

Effect of Floc Size on Specific Cake Resistance

The results in Fig. 4a, obtained at a low TMP of 6–7 kPa, show that larger flocs have smaller α_c values in accord with the expected trends of the Carman-Kozeny equation (Eq. 3). However α_c values at floc sizes of 10 and 50 microns differ by a factor of about 7 whereas Eq (3) predicts a factor of 25.

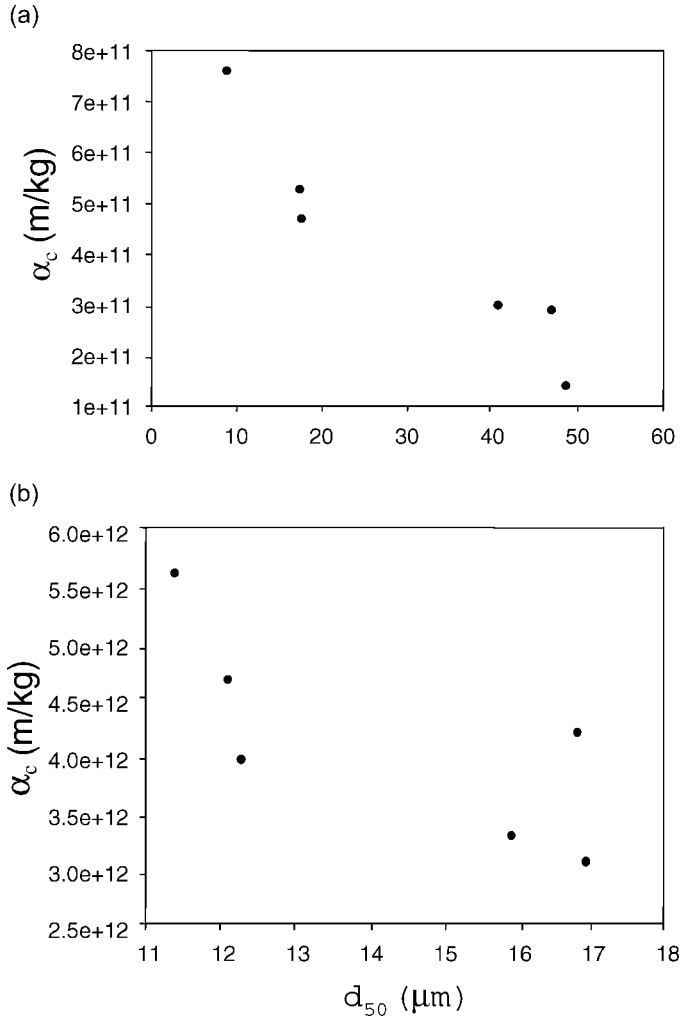

Figure 4. Variation of α_c as a function of mean floc size for a) TMP of 6–7 kPa and b) TMP of 50 kPa.

The behavior shown in Fig. 4a may be attributable to both inter- and intra-floc porosity effects and suggests that at the low TMP the structure and permeability of the floc is influencing the cake permeability. The trends in Fig. 4b (50 kPa) are closer to the Carman-Kozeny expectation of $\alpha_c \propto (d_p)^{-2}$

possibly due to some restructuring of flocs at this higher pressure with a likely reduction in intra-floc porosity, as discussed next.

Effect of Floc Structure on Specific Cake Resistance

Figure 4(a–c) shows the relationships between floc structure and specific cake resistance. The x-axis uses a qualitative description of structure for the larger flocs and the d_F values for the smaller flocs. The diameter of each circle is indicative of the measured d_{50} of each floc from SALLS (d_{50} of the smallest and largest flocs are 11.4 and 17.0 μm in Fig. 4a, 8.1 and 13.9 in Fig. 4b, and 40.6 and 48.5 in Fig. 4c, respectively). The data in Fig. 5a were obtained for TMPs of 50 kPa in all cases, whereas for Figs. 4b and 4c the resistances were obtained over a range of TMPs, and the α_c at 50 kPa was obtained by interpolation.

Floc structure effects appear to be significant for cakes made of small flocs (8.1–17 μm) (with α_c increasing as floc compactness increases) but negligible for cakes made of large flocs (40.6–48.5 μm). These results are in accord with the trends predicted by Eq. (5) and illustrated by Fig. 1. In effect the high-permeability cakes formed of 40 μm floc will be little influenced by intra-floc permeability, but 10 μm floc would tend to form cakes with an order of magnitude lower permeability and therefore be influenced by floc porosity. These trends could be further modified by compressibility effects (see the next section).

Effect of Floc Size on Cake Compressibility

The "cake-averaged porosity," ε_c, can be considered to be a composite of both inter- and intra-floc porosity, as well as averaging any porosity gradients[18,20] in the cake. In this work it was estimated from the measured values of α_c and the primary particle size using the Carman-Kozeny equation. Initial calculations showed that porosities were relatively high (>0.5) which means that the Kozeny constant in Eq. (3) is likely to be a function of porosity. To allow for this, use was made of the following correlation obtained from the data of Brinkman,[5] for $\varepsilon_c > 0.6$,

$$K' = 1.88 \times 10^{-3} e^{8.53\varepsilon_c} + 3.90 \tag{8}$$

Thus estimated cake-averaged porosities vs. TMP were calculated via Eq. (3) and Eq. (8) using experimental α values and the primary particle size as the particle size in Eq. (3). Estimated average values of porosity at different

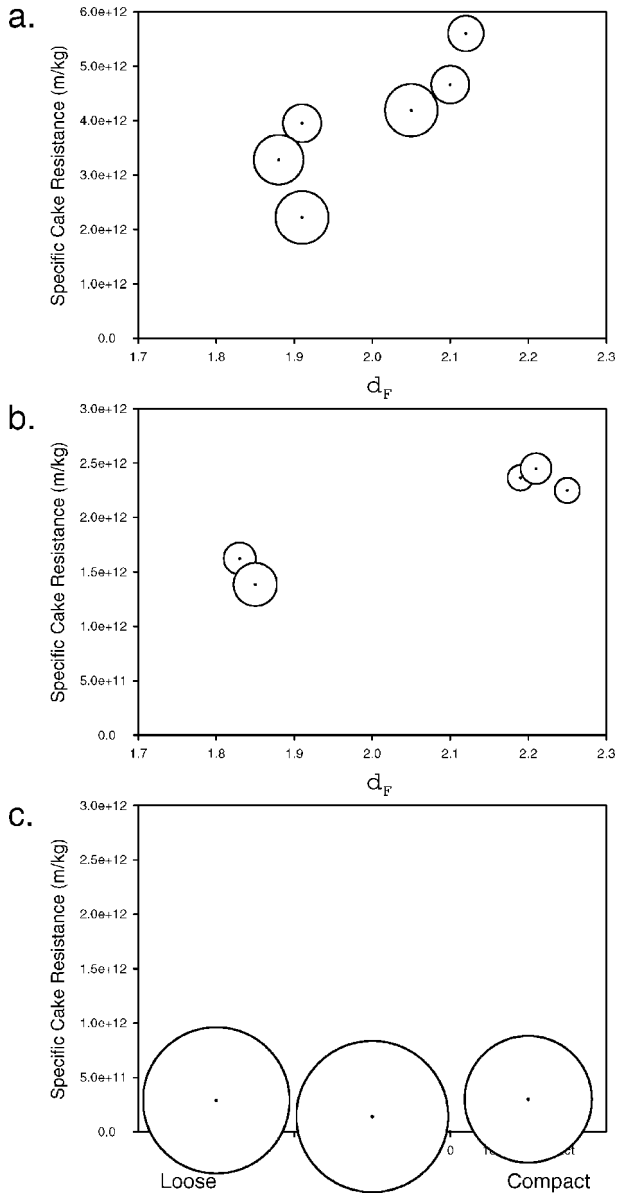

Figure 5. Variation of α_c as a function of structure of hematite flocs of various sizes. Circle size depicts floc d_{50} size.

TMPs are shown in Fig. 6 (floc sizes from 8.05–48.5 μm). Porosity is seen to decrease markedly on increase in TMP, presumably as a result of compaction effects. However, provided TMP is kept relatively low (say < 15 kPa) a high cake-averaged porosity is maintained. The magnitudes of ε_c lie between the typical random-sphere cake porosity (about 0.4) and the typical aggregate porosity [Eq. (4) with $d_F = 2.0$, gives ε_a of 0.9 to 0.99 for r_a/r_p of 10 to 100].

The effect of floc size on cake compressibility is shown in Fig. 7. For higher TMP conditions (> 60 kPa), the cake-averaged porosity exhibits a strong size dependence with larger floc sizes yielding higher cake-average porosities. This result may indicate formation of relatively impermeable assemblages (as a result of significant compaction) with flux controlled by interaggregate flow (i.e., flow around compressed flocs). In comparison, the data at low TMP show less size dependence, which suggests that floc collapse is limited and intraaggregate flow is important. These trends are in accord with the observations of Antelmi et al.[13] on the effects of pressure on cake structure.

Effect of Floc Structure on Cake Compressibility

The results so far suggest that filter cakes developed from fractal aggregates can be compressed with their relative compressibility dependent on

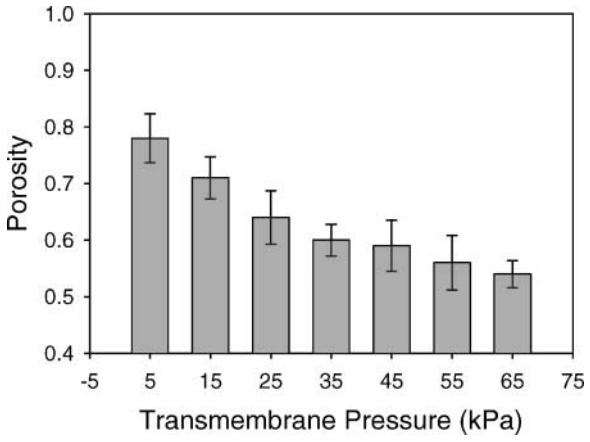

Figure 6. Effect of transmembrane pressure on cake porosity calculated from experimental specific cake resistance using the Carman-Kozeny equation and the Brinkman correction.

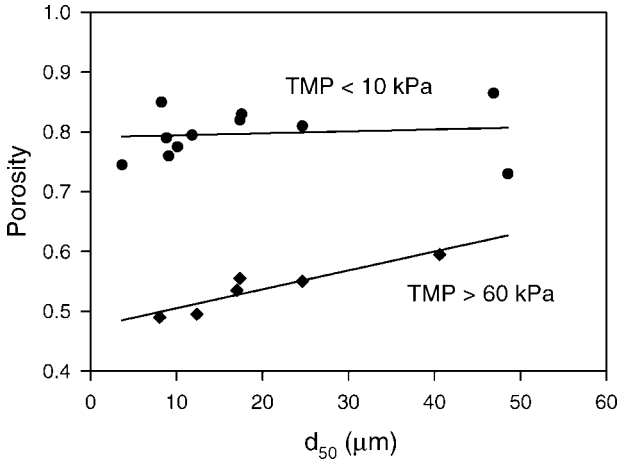

Figure 7. Calculated cake porosity as a function of median floc size at low TMP (< 10 kPa) and raised TMP (> 60 kPa).

floc size. However, it would be expected that cakes generated from loose aggregates may be more susceptible to compression effects than compact aggregates, particularly at higher TMPs. This issue is examined in Fig. 8(a–c), which shows the effects of TMP on the specific cake resistance of cakes formed from flocs of various size and structure. The compressibility values (n) are also shown.

In general, cakes made of small, loose flocs (Fig. 8a) exhibit higher compressibility at the higher TMP whereas cakes made of small, compact flocs (Fig. 8b) are less compressible. Specifically Fig. 8a shows that a critical TMP (> 60 kPa) must be reached before the cakes formed from small, loose flocs undergo significant compression ($n = 0.8$ for runs 30a and b) compared to the small, compact floc ($n < 0.5$ for runs 180a and 180b). Again the results tie in with the cake collapse observations of Antelmi et al.[13]

The results in Fig. 8c show low specific resistance for cakes made of large flocs. As discussed earlier, their low resistance might be expected as a result of both high inter-floc and intra-floc porosity for large flocs. The compressibility values of these large floc cakes are high for both loose (30c) and more compact (180c and d) flocs, but relatively low specific resistances are maintained. These results confirm that cakes made from large flocs are highly permeable irrespective of whether the flocs are loose or compact.

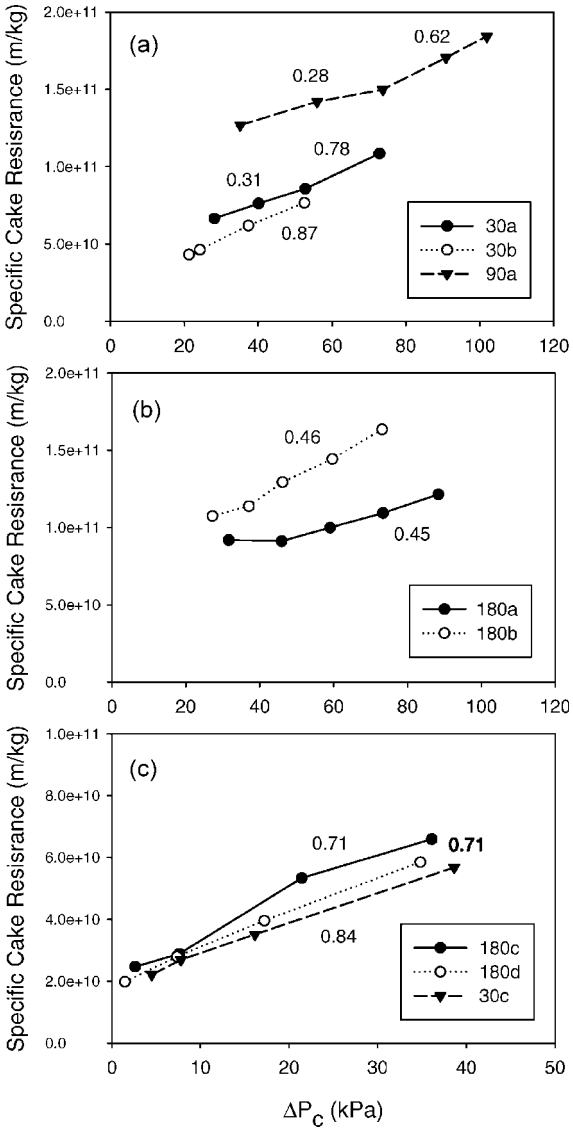

Figure 8. Specific cake resistance as a function of transcake pressure drop. Also shown are the compressibility values (n) for each set of data points [obtained using Eq. (7)]. Cakes in (a) were formed from small, loose flocs whereas those in (b) were formed from small, compact flocs. Large flocs of varying structure (see Table 1) were used in (c).

CONCLUSIONS

The effects of floc size and structure (as characterized by the fractal dimension) are in qualitative agreement with a simple model based on the Carman-Kozeny equation. Larger flocs form cakes with large inter-floc permeability, which results in a significantly lower resistance than achieved for smaller flocs. Concomitantly, looser flocs (of low fractal dimension) are likely to form cakes with higher intra-floc porosity and lower resistance than a cake made of compact flocs of similar size. Our results confirm that there is an interplay between floc size and structure and that cakes formed of smaller flocs are more sensitive to floc structure effects than cakes of larger flocs.

Cake compression results indicate that compressibility is strongly influenced by trans-membrane pressure (TMP), particularly for smaller floc sizes. The deposition of highly porous aggregates onto the membrane results in the formation and maintenance of a highly porous cake layer, provided a low TMP (<10 kPa) is applied. Rapid compression of the cake occurs at higher TMPs (>60 kPa) as shown by the significantly lower porosity of the cake. Under high TMP conditions, the cake-averaged porosity exhibits a strong size dependence with larger floc sizes yielding higher porosities. This result may indicate formation of relatively impermeable assemblages (as a result of significant compaction) with resistance controlled by interaggregate permeability (i.e., flow around compressed flocs). In contrast, the reduced effect of floc size dependence on porosity at low TMP suggests that permeate flux involves a significant contribution of intraaggregate flow through (rather than around) the highly permeable flocs. From a practical perspective the results support the use of large, porous floc and operation at low TMP.

SYMBOLS

A	Membrane area
C	Particle concentration
d_{10}	Lower decile diameter of particles
d_{50}	Median diameter of particles
d_F	Fractal dimension
d_{floc}	Floc diameter
d_p	Primary particle diameter
J	Permeate flux (L/m^2 hr)
K''	Kozeny constant
m'	Cake mass per area
ΔP	Transmembrane pressure (kPa)

ΔP_c	Transcake pressure drop (kPa)
R_c	Cake resistance (m^{-1})
R_m	Membrane resistance (m^{-1})
r_a	Aggregate radius
r_p	Primary particle radius
α_c	Specific cake resistance(m/kg)
ε_c	Cake-average porosity
ε_a	Porosity of aggregates
ε_s	Cake porosity of hard spheres
μ	Fluid viscosity
ρ_p	Density of the particles

ACKNOWLEDGMENTS

This work was supported by the CRC for Water Quality and Treatment, a Centre established and supported under the Australian Government's Co-operative Research Centres Program. Material support from Millipore Australia is also acknowledged.

REFERENCES

1. Judd, S.J.; Hillis, P. Optimisation of combined coagulation and microfiltration for water treatment. Wat. Res. **2001**, *35* (12), 2895–2904.
2. Wiesner, M.R.; Laine, J.-M. Coagulation and membrane separation (Chapter 16). In *Water Treatment Membrane Processes*; Mallevialle, J., Odendaal, P.E., Wiesner, M.R., Eds.; American Water Works Association Research Foundation McGraw-Hill: New York, 1996; 16.1–16.12.
3. Laine, J.-M.; Vial, D.; Moulart, P. Status after 10 years of operation—overview of UF technology today. Proceedings of IWA Conference, Membranes in Drinking and Industrial Water Production, Paris 2000, Vol. 1, 17–26.
4. Carman, P.C. Fundamental principles of industrial filtration. Trans. Inst. Chem. Eng. **1938**, *16*, 168.
5. Brinkman, H.C. On the permeability of media consisting of closely packed porous particles. Appl. Sci. Res. **1948**, *1*, 81–86.
6. Hlavacek, M.; Remy, J.F. Simple relationships among zeta potential, particle size distribution, and cake specific resistance for colloid

suspensions coagulated from ferric chloride. Sep. Sci. Technol. **1995**, *30* (4), 549–563.
7. Wiesner, M.R.; Clark, M.M.; Mallevialle, J.L. Membrane filtration of coagulated suspensions. J. Environ. Eng. **1989**, *115* (1), 20–40.
8. Lin, M.Y.; Klein, R.; Lindsay, H.M.; Weitz, D.A.; Ball, R.C.; Meakin, P. The structure of fractal colloidal aggregates of finite extent. J. Colloid Interface Sci. **1990**, *137* (1), 263–280.
9. Khatib, K.; Rose, J.; Barres, O.; Stone, W.; Bottero, J.-Y. Physico-chemical study of fouling mechanisms of UF membranes on Biwa Lake (Japan). J. Memb. Sci. **1997**, *130*, 53–62.
10. Waite, T.D.; Schafer, A.I.; Fane, A.G.; Heuer, A. Colloidal fouling of ultrafiltration membranes: impact of aggregate structure and size. J. Colloid Interface Sci. **1999**, *212*, 264–274.
11. Pignon, F.; Magnin, A.; Piau, J.M.; Cabane, B.; Aimar, P.; Meireles, M.; Linder, P. Structural characterization of deposits formed during frontal filtration. J. Memb. Sci. **2000**, *174*, 189–204.
12. Hu, X.; Luo, Q.; Wang, C. Investigations on the state of water in a flocculated filter cake. Sep. Sci. Technol. **1996**, *31* (13), 1877–1887.
13. Antelmi, D.; Cabane, B.; Meireles, M.; Aimar, P. Cake collapse in frontal filtration. Langmuir **2001**, *17* (22), 7137–7144.
14. Guan, J.; Amal, R.; Waite, T.D. Effect of aggregate size and structure on specific cake resistance of biosolids filter cakes. Water Sci. Technol. **2001**, *44* (10), 215–220.
15. Matijevic, E.; Scheiner, P. Ferric hydrous oxide sols III. J. Colloid Interface Sci. **1978**, *63* (3), 509–524.
16. Amal, R.; Raper, J.A.; Waite, T.D. Effect of fulvic acid adsorption on the aggregation kinetics and structure of hematite particles. J. Colloid Interface Sci. **1991**, *151*, 244–257.
17. Bushell, G.; Amal, R. Measurement of fractal structure of polydispersed particles using small angle light scattering. J. Colloid Interface Sci. **2000**, *221*, 186–194.
18. Tiller, F.M.; Kwon, J.H. Role of porosity in filtration: XIII. Behavior if highly compactible cakes. AIChE J. **1998**, *44*, 2159–2167.
19. Parameshwaran, K.; Fane, A.G.; Cho, B.D.; Kim, K.J. Analysis of microfiltration performance with constant flux processing of secondary effluent. Water Res. **2001**, *35* (1), 4349–4358.
20. Hwang, K.J.; Lui, H.C.; Lu, W.M. Local properties of cake in cross-flow MF of submicron particles. J. Membr. Sci. **1998**, *138*, 181–192.